

Journal of

[www. biophotonics-journal.org](http://www.biophotonics-journal.org)

BIOPHOTONICS

 WILEY-VCH

REPRINT

FULL ARTICLE

Retrieving skin properties from *in vivo* spectral reflectance measurements

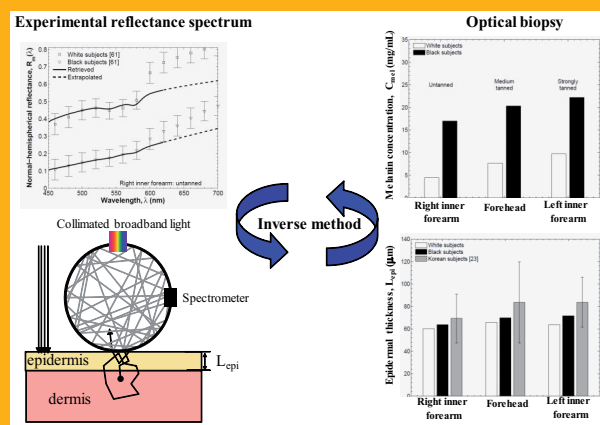
Dmitry Yudovsky and Laurent Pilon*

University of California, Los Angeles, Henry Samueli School of Engineering and Applied Science, Mechanical and Aerospace Engineering Department, Biomedical Inter-Department Program, Los Angeles, CA 90095-1597

Received 21 May 2010, revised 18 July 2010, accepted 19 July 2010
Published online 4 August 2010

Key words: skin optics, reflectance spectroscopy, two-layer tissue model, optical biopsy, non-invasive tissue diagnosis

A previously developed inverse method was applied to *in vivo* normal-hemispherical spectral reflectance measurements taken on the inner and outer forearm as well as the forehead of healthy white Caucasian and black African subjects. The inverse method was used to determine the thickness and melanin concentration in the epidermis, dermal blood volume fraction and oxygen saturation, and skin's spectral scattering coefficient. It was established that changes in melanin concentration due to racial difference and tanning, and differences in epidermal thickness and blood volume with anatomical location were detectable. The retrieved values were also consistent with independent measurements reported in the literature. The same method could be used for optical diagnosis of pathologies affecting the structure and pigmentation of human skin.



1. Introduction

Reflectance spectroscopy has found many applications in non-invasive monitoring of biological tissues [1–7]. This technique investigates tissue structure, chromophore concentration, and health by measuring its optical properties. Typical spectroscopic techniques are based on the assumption that tissue is homogeneous and that properties are independent of depth [6–13]. In reality, most bodily organs such as skin are protected by a thin lining called the epithelial layer [14]. While the organ is typically composed of cells and connective tissues and per-

fused with blood vessels and nerves, the protective epithelial layer is bloodless and consists of structured cell layers with little connective tissue [14].

Skin is the largest organ of the human body representing a total surface area of approximately 1.8 m² and a total weight of approximately 11 kg for adults [15]. The skin consists of two main layers, namely the epidermis and dermis separated by the basement membrane and resting on the subcutaneous fat layer [15]. The topmost layer of the epidermis is called the stratum corneum and is composed of dead cells embedded in a lipid matrix. The rest of the epidermis is mainly composed of keratinocytes,

* Corresponding author: e-mail: pilon@seas.ucla.edu, Phone: +1 (310)-206-5598, Fax: +1 (310)-206-4830

melanocytes, and Langerhans [15]. Melanocytes synthesize melanin which absorbs strongly in the ultraviolet (UV) part of the spectrum. Melanin is contained in organelles known as melanosomes which are distributed throughout the epidermis [15]. Melanin concentration in the epidermis was assumed to range between 0 and 100 mg/mL of epidermal thickness [16]. On the other hand, epidermal thickness varies with anatomical location, age, and health and ranges between 20 and 150 μm [17–21].

The dermis, located beneath the epidermis, is responsible for the skin's pliability, mechanical resistance and temperature control. The dermis is primarily composed of collagen fibers perfused by nerves, capillaries, and blood vessels but also contains elastin, fibroblasts, and Schwann and endothelial cells [20, 22]. The thickness of the dermis ranges between 450 and 1000 μm [23, 24]. Approximately half of the blood volume is occupied by erythrocytes (red blood cells) which are responsible for oxygen transfer from the lungs to the rest of the body [25]. Erythrocytes are composed mainly of hemoglobin molecules which reversibly bind to oxygen molecules in the lungs to form oxyhemoglobin. Hemoglobin is known as deoxyhemoglobin once it has released its oxygen molecules. Depending on body location and tissue health, the volume of blood in the dermis ranges between 0.2% and 7% [18, 26]. The ratio of oxyhemoglobin molecules to the total number of hemoglobin molecules in the blood is the so-called oxygen saturation denoted by SO_2 . Hemoglobin absorption dominates the absorption of visible light by the dermis [15, 20, 22]. Furthermore, the spectral absorption coefficient of oxyhemoglobin differs significantly from that of deoxyhemoglobin. Thus, the color of the dermis depends of the local oxygen saturation of the blood flowing through it.

The objective of the present study is to demonstrate the capability of reflectance spectroscopy to rapidly, non-invasively, and simultaneously determine the epidermal melanin concentration and thickness, dermal blood volume and oxygen saturation, as well as scattering coefficient from *in vivo* spectral reflectance measurements.

2. Background

2.1 Reflectance spectroscopy of human skin

Quantitative assessment of tissue pigmentation by melanin and blood can be used to detect a wide variety of medical conditions. Acute and long term inflammation caused by infection, irritation, or ulceration, for example, can lead to hyperpigmentation [27, 28]. In fact, hyperpigmentation is typical in areas

surrounding venous ulcers and other chronic wounds due to extravasation of red blood cells into the dermis, collections of hemosiderin within macrophages, and melanin deposition [27, 29–31]. Alternatively, extreme inflammation may eventually destroy melanocytes in the epidermis resulting in hypopigmentation in and around the ulcer site after ulcer healing [28]. Additionally, Dwyer et al. [32] showed that increased melanin concentration correlates with the risk of melanoma skin cancer in 19 to 20 year old subjects of northern European ancestry. Kono et al. [33] used reflectance spectroscopy to estimate blood volume fraction during port-wine stains and acne laser treatments to determine the intensity of a laser pulse. Additionally, hyperspectral imaging in the visible and near-infrared parts of the spectrum has been used to determine the spatial distribution of oxygen saturation in the human skin [12]. This technique has been applied clinically to study diabetic neuropathy [34] and predict the healing potential of diabetic foot ulcers [4, 35].

Epidermal thickness varies naturally with age, gender, and body location [23, 36–38]. It may also increase or decrease due to external stimuli. For example, UV exposure of human skin has been shown to increase the epidermal thickness in addition to increasing its melanin content [39, 40]. On the contrary, smoking has been shown to decrease epidermal thickness [36]. Epidermal thickness can be measured reliably with punch biopsy whereby a sample of the skin is removed and analyzed *ex vivo* [23, 36, 40]. However, this invasive and destructive technique can be painful. Alternatively, non-invasive measurements of epidermal thickness can be made with techniques such as optical coherent tomography or ultrasound [41, 42]. However, these techniques are primarily sensitive to scattering of light and sound, respectively, by the tissue's macrostructures and therefore cannot be used to determine the tissue's chromophore concentration(s) easily [43, 44].

2.2 Modeling reflectance of human skin

Multilayer optical models have been proposed to investigate the effects of tissue structure on its reflectance spectrum [13, 45–47]. The governing equation for light transfer through tissue can be solved using Monte Carlo [11, 46, 47], finite element [45], or discrete ordinates [48] methods, for example. However, these solution methods can be computationally intensive and time consuming and therefore cannot be used in real-time clinical applications where the inverse problem requires that the forward radiative transfer problem be solved numerous times [25]. Alternatively, various computationally efficient models have been proposed approximating tissue as a finite

slab supported by a semi-infinite layer corresponding to the epithelium and the organ, respectively. The diffusion approximation has often been used to model light transfer through tissue [49–52]. It can be solved rapidly and produces accurate estimates of the tissue's reflectance spectrum if the tissue exhibits significant scattering [53, 54]. However, strongly pigmented skin can absorb significantly and so the diffusion approximation may not be valid and/or give inaccurate predictions [25]. Instead, semi-empirical models of light transfer have been developed to accelerate computation without significant loss of accuracy [55–60]. Recently, Yudovsky and Pilon [61] developed an inverse method based on a semi-empirical model for the diffuse reflectance from two-layer media subjected to collimated and normally incident light [56]. The inverse method could determine the epidermal thickness, the chromophore concentrations in both epidermis and dermis, and their scattering coefficient from normal-hemispherical diffuse reflectance spectra of human skin that was numerically generated using Monte Carlo simulations.

2.3 Spectral reflectance measurements of *in vivo* human skin

Reflectance measurements from human skin have been reported in the Refs. [62–65]. Kuppenheim and Heer [65] measured the normal-hemispherical reflectance between 440 and 1000 nm on numerous subjects of white Caucasian and black African descent featuring lightly pigmented and strongly pigmented skin, respectively. The reflectance data reported in

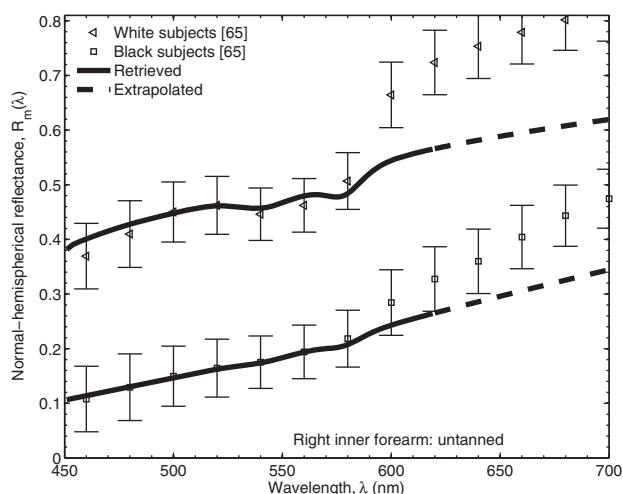


Figure 1 Average normal-hemispherical reflectance measured from the untanned right inner forearm of white and black subjects [65]. The solid line represents the retrieved reflectance between 440 and 620 nm.

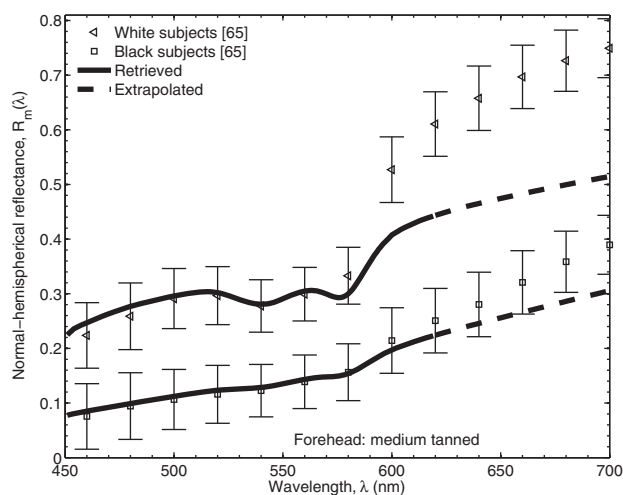


Figure 2 Average normal-hemispherical reflectance measured from the medium tanned forehead above the left eye of white and black subjects [65]. The solid line represents the retrieved reflectance between 440 and 620 nm.

Ref. [65] agrees with that reported in Refs. [62–64]. Their measurements consisted of (i) illuminating a circular spot of skin, 1 inch in diameter, with normally incident and monochromatic light and (ii) collecting the hemispherical reflectance with an integrating sphere [65]. The subject population consisted of 50 male and 21 female white participants and 21 male and 21 female black participants. All subjects were healthy adults but their age range was not specified. Reflectance measurements were performed at the end of the summer season at three locations: (i) the right inner forearm, (ii) the forehead over the left eye, and (iii) the left outer forearm.

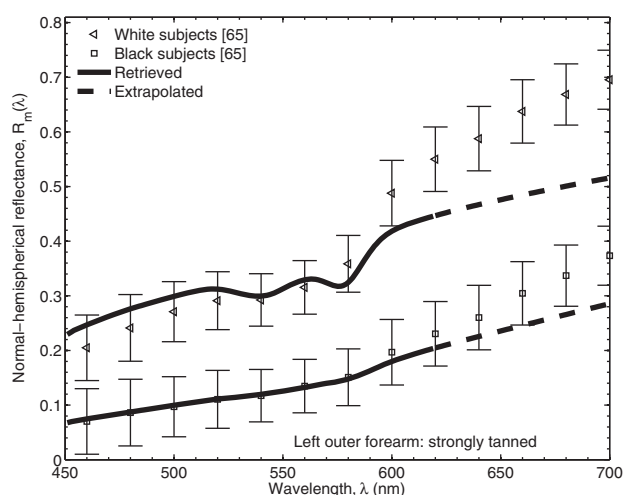


Figure 3 Average normal-hemispherical reflectance measured from the strongly tanned left outer forearm of white and black subjects [65]. The solid line represents the retrieved reflectance between 440 and 620 nm.

Table 1 Lower and upper bounds and initial guesses used for determining the biological properties of human skin from reflectance measurements.

Biological Property	Symbol	Range	Initial guess	Reference
Melanin concentration	C_{mel}	0 to 100 mg/mL	Eq. (10)	[18, 32, 85]
Epidermal thickness	L_{epi}	20 μm to 150 μm	150 μm	[17–21]
Blood volume fraction	f_{blood}	0.2% to 7%	2%	[18, 25]
Oxygen saturation	SO_2	20% to 100%	50%	[14]
Scattering constant	C	10^5 to 10^6 cm^{-1}	$5 \times 10^5 \text{ cm}^{-1}$	[18]
Scattering power constant	b	1.50		[18, 79]

These three sites had been subjected to low, medium, and high exposure to UV radiation, respectively, for both white and black subjects. Figures 1 through 3 show the averaged and standard deviation of the total hemispherical reflectance between 440 and 1000 nm for the three locations considered and for both populations of subjects with lightly and darkly pigmented skin as reported in Table 1 of Ref. [65]. The standard deviation represents the biological variability in tissue properties within the population considered and not the experimental error associated with the measurement of tissue reflectance and the experimental noise. Note also that the distribution of reflectance values about the mean was not normal but rectangular [65].

In the present study, our inverse method [61] was applied to *in vivo* spectral reflectance collected by Kuppenheim and Heer [65] in order to estimate (i) changes in tissue pigmentation due to racial differences or exposure to sunlight as well as differences in (ii) blood volume fraction in the dermis, (iii) epidermal thickness from one anatomical location to another, and (iv) the tissue scattering coefficient. These measurements were used in this study to assess the capability of our inverse method [61] to retrieve the physiological properties of skin from *in vivo* experimental data gathered from a variety of human skin [65] as opposed to numerically generated reflectance spectra. We chose to analyze this dataset because measurements were carefully performed and described and the population considered (i) was large and described in details, (ii) had very different skin complexion (white or black), (iii) featured different locations and sun exposures.

3. Methods

3.1 Optical model of human skin

In the present study, skin was approximated as a plane-parallel slab of thickness L_{epi} , representing the epidermis, characterized by absorption coefficient

$\mu_{a,\text{epi}}(\lambda)$ and transport scattering coefficient $\mu_{s,\text{tr}}(\lambda)$ along with a constant index of refraction $n_1 = 1.44$ in the visible part of the spectrum as reported in the Refs. [14, 20, 49–52, 57]. This top layer was supported by a semi-infinite sub-layer representing the dermis and characterized by $\mu_{a,\text{derm}}(\lambda)$, $\mu_{s,\text{tr}}(\lambda)$ and $n_2 = n_1$ [66]. The dermis was treated as a semi-infinite medium because it is typically thicker than 1 mm [14, 20] while the penetration depth of visible light in skin is approximately 1 mm [20, 23]. Thus, a negligible amount of visible light reaches the subcutaneous fat layer. The incident light source was assumed to be collimated, monochromatic, and normally incident. The air-skin interface and the interfaces between the skin layers are inherently rough [13]. However, for the sake of simplicity but also to be consistent with assumptions made while retrieving the skin properties, the skin-air interface and the interfaces between the skin layers were assumed to be optically smooth.

Absorption in the epidermis is mainly due to melanin and flesh. Thus, the absorption coefficient of the epidermal layer $\mu_{a,\text{epi}}(\lambda)$ was expressed as [16, 67],

$$\mu_{a,\text{epi}}(\lambda) = \varepsilon_{\text{mel}}(\lambda) C_{\text{mel}} + \mu_{a,\text{back}}(\lambda) \quad (1)$$

where C_{mel} is the concentration of melanin in the epidermis measured in mg/mL and $\mu_{a,\text{back}}(\lambda)$ is the background absorption coefficient of human flesh given by [68],

$$\mu_{a,\text{back}}(\lambda) = 7.84 \times 10^8 \lambda^{-3.255} \quad (2)$$

where λ is expressed in nanometers and $\mu_{a,\text{back}}(\lambda)$ is expressed in cm^{-1} . The spectral absorption coefficient of pure melanin in solution $\varepsilon_{\text{mel}}(\lambda)$ was reported by Sanra and Sealy [69] in units of $\text{cm}^{-1}/(\text{mg/mL})$ between 250 and 1,000 nm and used in the present study. The absorption coefficient of the dermis is dominated by blood absorption [15, 20, 22] and can be written as [26, 70],

$$\mu_{a,\text{derm}}(\lambda) = f_{\text{blood}} \mu_{a,\text{blood}}(\lambda) + \mu_{a,\text{back}}(\lambda) (1 - f_{\text{blood}}) \quad (3)$$

where f_{blood} is the volume fraction of the dermis occupied by blood. The absorption coefficient of blood is given by $\mu_{a,\text{blood}}(\lambda) = \mu_{a,\text{oxy}}(\lambda) + \mu_{a,\text{deoxy}}(\lambda)$ where the absorption coefficient of oxyhemoglobin $\mu_{a,\text{oxy}}(\lambda)$ and deoxyhemoglobin $\mu_{a,\text{deoxy}}(\lambda)$ were found in the literature [25] as a function of oxygen saturation SO_2 so that $\mu_{a,\text{oxy}}(\lambda) = \text{SO}_2 C_{\text{heme}} \varepsilon_{\text{oxy}}(\lambda)/66,500$ and $\mu_{a,\text{deoxy}}(\lambda) = (1 - \text{SO}_2) C_{\text{heme}} \varepsilon_{\text{deoxy}}(\lambda)/66,500$ [25]. Here, $C_{\text{heme}} = 150 \text{ g/L}$ is the average hemoglobin concentration in blood and $\varepsilon_{\text{oxy}}(\lambda)$ and $\varepsilon_{\text{deoxy}}(\lambda)$ refers to the spectral absorption coefficient of oxyhemoglobin and deoxyhemoglobin, respectively [19, 26, 70–74].

The spectral scattering coefficients of the epidermis and dermis were assumed to be identical [66] and given by [75–78],

$$\mu_{s,\text{tr}}(\lambda) = C \left(\frac{\lambda}{\lambda_0} \right)^{-b} \quad (4)$$

where $\lambda_0 = 1 \text{ nm}$ was introduced to ensure unit consistency. The scattering power constant b was assumed constant and equal to 1.50 as reported in the literature for all locations while C was assumed to range between 10^5 to 10^6 cm^{-1} [18, 78, 79]. Equations (1) through (4) have been used successfully in the literature to describe the optical properties of human epidermis and dermis *in vivo* [25].

3.2 Inverse method

Overall, the optical properties of skin depend on the property vector $\vec{a} = \langle C_{\text{mel}}, L_{\text{epi}}, f_{\text{blood}}, \text{SO}_2, C \rangle$. In addition, the hemispherical diffuse reflectance, denoted by $R_d(\vec{a}, \lambda)$, refers to the fraction of the incident spectral irradiation that re-emerges from the skin after multiple scattering events integrated over the external hemisphere. Yudovsky and Pilon [56] developed a rapid and accurate expression for $R_d(\vec{a}, \lambda)$ accounting for the distinct optical properties of the epidermis and dermis and given by [56],

$$R_d(\vec{a}, \lambda) = R^* [R_-(n_1, \omega_{\text{tr,epi}}) - R_-(n_1, \omega_{\text{tr,derm}})] + R_-(n_1, \omega_{\text{tr,derm}}) \quad (5)$$

where $\omega_{\text{tr,epi}}(\lambda)$ and $\omega_{\text{tr,derm}}(\lambda)$ are the transport single scattering albedos of the epidermis and dermis, respectively and $\omega_{\text{tr}}(\lambda)$ is defined as $\omega_{\text{tr}}(\lambda) = \mu_{s,\text{tr}}(\lambda)/[\mu_a(\lambda) + \mu_{s,\text{tr}}(\lambda)]$. The reduced reflectance R^* is a function of a single semi-empirical parameter α and expressed as [56],

$$R^* = \frac{\tanh(Y_{\text{epi}})}{1/\alpha + (1 - 1/\alpha) \tanh(Y_{\text{epi}})} \quad (6)$$

The parameter Y_{epi} is the modified optical thickness defined as $Y_{\text{epi}} = \zeta[\mu_{a,\text{epi}}(\lambda) + \mu_{s,\text{tr}}(\lambda)] L_{\text{epi}}$ [80]. The

parameter ζ and α were given as polynomial expressions in terms of $\omega_{\text{tr,epi}}(\lambda)$ and $\omega_{\text{tr,derm}}(\lambda)$, respectively [56]. The function $R_-(n_1, \omega_{\text{tr}})$ appearing in Eq. (5) is the diffuse reflectance of a semi-infinite homogeneous layer, with transport single scattering albedo $\omega_{\text{tr}}(\lambda)$ and index of refraction n_1 given by [56],

$$R_-(n_1, \omega_{\text{tr}}) = [1 - \varrho_{01}(n_1)] [1 - \hat{\varrho}_{10}(n_1, \omega_{\text{tr}})] \times \frac{\hat{R}_d(\omega_{\text{tr}})}{1 - \hat{\varrho}_{10}(n_1, \omega_{\text{tr}}) \hat{R}_d(\omega_{\text{tr}})} \quad (7)$$

where $\varrho_{01}(n_1)$ is the normal-normal specular (or Fresnel) reflection due to mismatch in the refraction index at the tissue/air interface and defined as,

$$\varrho_{01}(n_1) = \left(\frac{n_1 - n_0}{n_1 + n_0} \right)^2 \quad (8)$$

where n_0 and n_1 are the refraction indices of air ($n_0 = 1$) and the tissue, respectively. Expressions for $\hat{\varrho}_{10}(n_1, \omega_{\text{tr}})$ and $\hat{R}_d(\omega_{\text{tr}})$ were given in Eqs. (26) and (27) of Ref. [56], respectively. The relative error between the semi-empirical model and Monte Carlo simulations was typically around 3% and never more than 8% for the optical properties of skin in the visible considered in this study [56].

Recently, Yudovsky and Pilon [61] developed an inverse method based on the above model and numerical generated diffuse reflectance spectra. Here, the goal of the inverse problem was to estimate the vector \vec{a} from the measured reflectance $R_m(\lambda)$. This was achieved by finding an estimate vector \vec{a} that minimized the difference between the measured normal-hemispherical reflectance $R_m(\lambda)$ and its estimate $R_e(\vec{a}, \lambda)$, in the least squares sense. Iterative minimization was performed with the Levenberg-Marquardt algorithm and implemented in MATLAB[®]. Details about the implementation of the inverse method are available in Ref. [61].

The experimental reflectance spectra $R_m(\lambda)$ used in the present study were measured *in vivo* by Kuppenheim and Heer [65] as previously described. However, the model developed by Yudovsky and Pilon [56] neglected Fresnel reflection. To simulate experimental measurements reported by Kuppenheim and Heer [65], the specular reflectance for normal incidence and optically smooth surface was added to $R_d(\vec{a}, \lambda)$ to yield,

$$R_e(\vec{a}, \lambda) = R_d(\vec{a}, \lambda) + \varrho_{01}(n_1) \quad (9)$$

where the second term on the right-hand side of Eq. (9) evaluated for $n_1 = 1.44$ is equal to 0.0325 which is often much smaller than $R_d(\vec{a}, \lambda)$.

Initial guesses for melanin concentration in the epidermis C_{mel} were determined from an empirical relationship suggested by Kollias and Baquer [16],

$$C_{\text{mel}} = -1.67 - 7936s_{620,720} \quad (10)$$

where $s_{620,720}$ is the slope of a linear fit to the function $-\ln[R_m(\lambda)]$ for wavelength λ between 620 and 720 nm. The value of C_{mel} was constrained to be between the physiologically reasonable values of 0 and 100 mg/mL during the iterative minimization. The range and initial guess for all other parameters are summarized in Table 1. The inverse method was applied to reflectance data between 440 and 620 nm [65]. Indeed, beyond 600 nm, the accuracy of semi-empirical model of tissue reflectance [56] used in the present inverse method [61] diminishes due to weak absorption by melanin and hemoglobin resulting in a transport single scattering albedo approaching unity. However, the semi-empirical model is valid for ω_{tr} less than 0.99. Tissue spectroscopy techniques based on the diffusion approximation [53] can accurately model light transfer through skin for wavelengths beyond 600 nm but have been shown to perform poorly in for wavelengths less than 600 nm where absorption by melanin and hemoglobin is strong [54].

4. Results and discussion

Figures 1 through 3 show the measured (symbols) [65] and reconstructed (solid line) reflectance spectra as a function of wavelength between 440 and 700 nm. The reconstructed reflectance $R_e(\vec{a}, \lambda)$ for wavelengths greater than 620 nm is shown in dashed line for reference only and was not considered during inversion [61]. The reconstructed reflectance spectra $R_e(\vec{a}, \lambda)$ matched the average measured reflectance $R_m(\lambda)$ within the standard deviation for all locations and for both populations. In fact, for wavelengths lower than 600 nm, the absolute difference between $R_e(\vec{a}, \lambda)$ and $R_m(\lambda)$ was less than 0.05 for all spectra considered. The values of C_{mel} , L_{epi} , f_{blood} , SO_2 and C determined for the (i) right inner forearm, (ii) forehead, and (iii) left outer forearm for

both populations considered are summarized in Table 2 and Figure 4.

Differences in melanin pigmentation occurred due to racial differences and/or exposure to UV light. For both populations considered, the right inner forearm was the least tanned location while the forehead and left outer forearm were the medium and most tanned locations, respectively. Figure 4a shows estimated values of C_{mel} from the right inner forearm, forehead, and left outer forearm. At these locations, it was found to be 4.41, 7.63, and 9.72 mg/mL for white subjects and 17.9, 20.2, and 22.2 mg/mL for the black subjects. For white subjects, the left outer forearm and forehead exhibited an increase in C_{mel} of 5.30 and 3.22 mg/mL, respectively, over the right inner forearm. It is interesting to note that the value of C_{mel} for black subjects calculated for the left outer forearm and forehead increased by almost identical amounts compared to the right inner forearm at 5.20 and 3.33 mg/mL, respectively. Thus, changes in melanin concentration caused by race and tanning can be detected by the present method.

Moreover, estimates of epidermal thickness L_{epi} from the inner and outer forearms and the forehead were, respectively, 60.1, 63.6, and 65.8 μm among the white subjects and 63.8, 71.6, and 69.8 μm for the black subjects as illustrated in Figure 4b. These values were consistent with those reported in the Refs. [23, 36, 41]. Furthermore, values of L_{epi} reported for skin of lightly versus strongly pigmented subjects were similar despite the very large difference in melanin concentration from one group to the other. In fact, Gambichler et al. [41] used optical coherence tomography to measure the epidermal thickness on the forearms and foreheads of 71 healthy Caucasian subjects aged 20 to 40 and 12 healthy Caucasian subjects aged 60 to 80. The authors reported that the epidermal thickness was on average 71 ± 7.8 and 62 ± 6.8 μm on the forearms and 72 ± 10 and 61 ± 7.4 μm on the foreheads of the younger and older populations, respectively.

Table 2 Biological properties determined from the average normal-hemispherical reflectance spectra reported in Ref. [65] and reproduced in Figures 1 to 3.

Site	White subjects (50 males, 21 females)			Black subjects (21 males, 21 females)		
	Right inner forearm	Forehead	Left outer forearm	Right inner forearm	Forehead	Left outer forearm
Tanning status	Untanned	Medium	Strong	Untanned	Medium	Strong
Melanin concentration C_{mel} (mg/mL)	4.41	7.63	9.72	17.0	20.3	22.2
Epidermal thickness L_{epi} (μm)	60.1	65.8	63.6	63.8	69.8	71.6
Blood volume f_{blood} (%)	1.01	2.06	0.78	0.90	1.98	1.41
Oxygen saturation SO_2 (%)	63.5	34.7	57.5	53.2	50.9	37.1
Scattering constant $C \times 10^{-5}$ (cm^{-1})	5.81	4.73	5.13	3.79	3.91	4.08

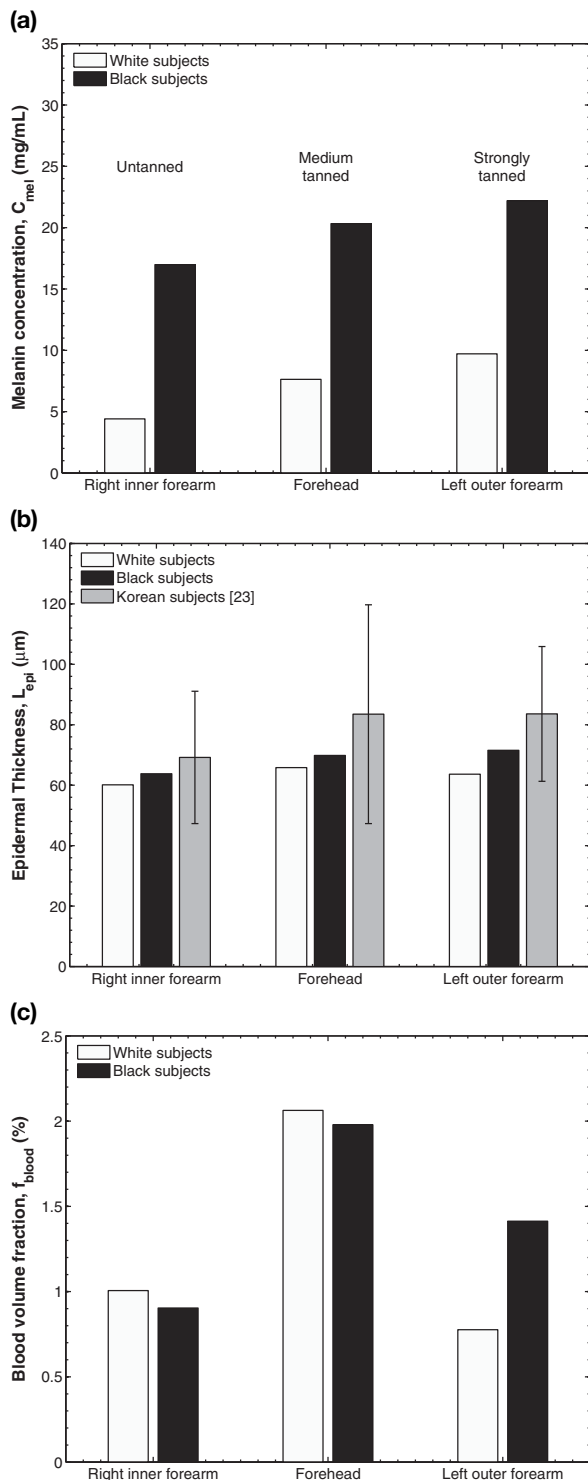


Figure 4 (a) Melanin concentration, (b) blood volume fraction, and (c) epidermal thickness determined from the average normal-hemispherical reflectance spectra on the right inner forearm, forehead, and left outer forearm of white and black subjects reported in Ref. [65] and reproduced in Figures 1 to 3. (c) also shows the average epidermal thickness and standard deviation at the same locations determined by Lee and Hwang [23] by biopsies.

In addition, Sandby-Møller et al. [36] performed biopsies on the shoulder, inner forearm and buttock of 71 healthy white volunteers and evaluated the thickness of the stratum corneum and cellular epidermis at each location by visual observation with a microscope. They reported that the epidermal thickness was $74.9 \pm 12.7 \mu\text{m}$ on the inner forearm. Lee and Hwang [23] also performed biopsies on various anatomical locations on 452 healthy Korean volunteers. They reported that the epidermal thickness on the inner and outer forearm and the forehead were 69.2 ± 21.9 , 83.5 ± 36.2 , and $93.6 \pm 22.3 \mu\text{m}$, respectively. The values of epidermal thickness retrieved in the present study are in good agreement with those reported by Lee and Hwang [23] and fall within the experimental uncertainty. Therefore, hemispherical reflectance combined with an inverse method can also retrieve the epidermal thickness within the experimental uncertainty of more sophisticated and sometimes invasive techniques.

Furthermore, blood volume in the dermis typically ranges between 0.2 and 7% depending on bodily location [25] and is larger in the forehead than in the forearm [81]. In the present study, similar trends were observed in the retrieved values of f_{blood} for both white and black subjects as suggested by Figure 4c. In fact, for the inner and outer forearm, f_{blood} was estimated to be 1.10 and 0.79% for lightly pigmented skin and 0.90 and 1.41% for strongly pigmented skin, respectively. As expected, estimates of blood volume in the forehead were larger at 2.06 and 1.98% for white and black subjects, respectively. In addition, estimates of SO_2 from the inner and outer forearm and the forehead were found to be 63.5, 57.5, and 34.7% for the lightly pigmented skin and 53.2, 37.1, and 50.9% for the strongly pigmented skin. These values of SO_2 fell within the normal range of SO_2 reported for healthy adult subjects [25]. In brief, estimates of both blood volume fraction and oxygen saturation could also be retrieved from the hemispherical reflectance of human skin. The retrieved values were within the normal range for healthy adults [25] and consistent between black and white subjects.

Finally, the retrieved values of the scattering power constant C ranged between approximately 3.5×10^5 and $6.0 \times 10^5 \text{ cm}^{-1}$ whereas the power-law constant b was assumed to be equal to 1.5. Note that varying b between 1.30 and 1.50 influenced the retrieved value of C but did not significantly alter the retrieved values of C_{mel} , f_{blood} , SO_2 , and L_{epi} . Furthermore, the reduced scattering coefficient $\mu_{s,tr}$ was essentially unaffected by the choice of b for wavelengths between 450 and 660 nm. Several studies have reported the spectral scattering coefficient of human dermis determined *in vitro* and *in vivo* by using various functional relationships between $\mu_{s,tr}$ and λ [78, 82–84]. Thus, it is more appropriate to

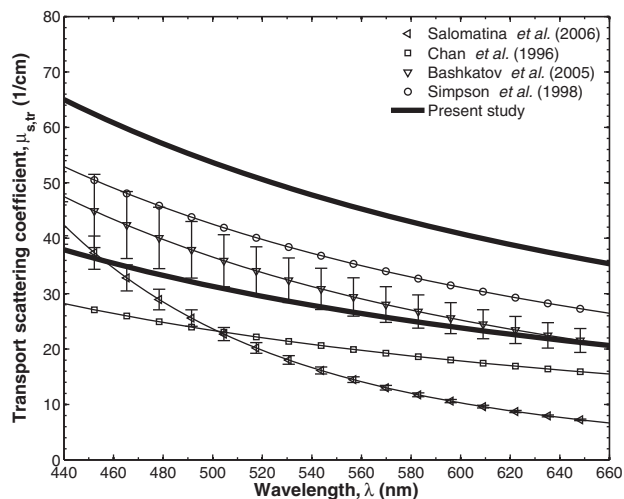


Figure 5 Transport scattering coefficient for λ between 440 and 660 nm reported in the Refs. [78, 82–84] and retrieved by the present method [Eq. (4) for $C = 3.5 \times 10^5$ and $6 \times 10^5 \text{ cm}^{-1}$].

compare the retrieved value of $\mu_{s,tr}$ between 440 and 660 nm with those reported in the literature. Figure 5 compares the scattering coefficient as a function of wavelength between 440 and 660 nm predicted by Eq. (4) for $b = 1.5$ and the lowest and highest values of C retrieved in the present study to values of $\mu_{s,tr}$ measured for human dermis as reported in the Refs. [78, 82–84]. It is evident that the shape and magnitude of $\mu_{s,tr}$ predicted by our method was in close agreement with this value determined by other studies.

5. Conclusion

This study applied a previously presented inverse method [61] to retrieve the epidermal melanin concentration and thickness, dermal blood volume and oxygen saturation, as well as the scattering coefficient of skin from normal-hemispherical reflectance spectra measured *in vivo* on the (i) right inner forearm, (ii) forehead over the left eye, and (iii) left outer forearm of groups of white and black subjects [65]. The differences in all the retrieved parameters due to racial differences, UV exposure, and anatomical location were consistent with independent experimental results reported in the literature. The proposed technique can be used to monitor changes in skin melanin volume fraction, epidermal thickness, and blood volume which can occur (a) in the normal course of aging, (b) due to UV exposure, or (c) as a result of diseases such as cancer, ulceration, or photodamage [23, 27, 28, 32, 36–40] as all of these affect the reflectance spectra of human skin [25].



Dmitry Yudovsky received his B.S. in Mechanical Engineering at the University of California, San Diego in 2006. He pursued his graduate studies at the University of California, Los Angeles where he received a M.S. and a Ph.D. in 2008 and 2010, respectively. His research interests include bio-

medical imaging, optical tissue modeling and non-invasive tissue health-monitoring.



Laurent Pilon received his B.S. and M.S. in Applied Physics in 1997 from the Grenoble Institute of Technology, France and a Ph.D. in Mechanical Engineering from Purdue University in 2002. He then joined the Mechanical and Aerospace Engineering Department at UCLA where he is now Associate Professor.

References

- [1] G. Zonios, A. Dimou, I. Bassukas, D. Galaris, A. Tso-lakidis, and E. Kaxiras, *J. Biomed. Opt.* **13**(1), 014017 (2008).
- [2] W. M. Kuebler, *J. Appl. Physiol.* **104**(4), 905–906 (2008).
- [3] R. L. P. van Veen, A. Amelink, M. Menke-Pluymers, C. van der Pol, and H. Sterenberg, *Phys. Med. Biol.* **50**(11), 2573–2581 (2005).
- [4] L. Khaodhiar, T. Dinh, K. T. Schomacker, S. V. Panasyuk, J. E. Freeman, R. Lew, T. Vo, A. A. Panasyuk, C. Lima, J. M. Giurini, T. E. Lyons, and A. Veves, *Diabetes Care* **30**(4), 903–910 (2007).
- [5] A. Torricelli, D. Contini, A. Pifferi, L. Spinelli, and R. Cubeddu, *Opto-Electron. Rev.* **16**(2), 131–135 (2008).
- [6] N. Tsumura, M. Kawabuchi, H. Haneishi, and Y. Miyake, *J. Imag. Sci. Technol.* **45**(5), 444–450 (2001).
- [7] N. Tsumura, H. Haneishi, and Y. Miyake, *J. Opt. Soc. Am. A* **16**(9), 2169–2176 (1999).
- [8] L. Kocsis, P. Herman, and A. Eke, *Phys. Med. Biol.* **51**(5), 91–98 (2006).
- [9] N. Tsumura, T. Nakaguchi, N. Ojima, K. Takase, S. Okaguchi, K. Hori, and Y. Miyake, *Appl. Opt.* **45**(25), 6626–6633 (2006).

- [10] E. Okada, M. Firbank, and D. T. Delpy, *Phys. Med. Biol.* **40**(12), 2093–2108 (1995).
- [11] M. Hiraoka, M. Firbank, M. Essenpreis, M. Cope, S. R. Arridge, P. Zee, and D. T. Delpy, *Phys. Med. Biol.* **38**(12), 1859–1876 (1993).
- [12] K. J. Zuzak, M. D. Schaeberle, E. N. Lewis, and I. W. Levin, *Analyt. Chem.* **74**(9), 2021–2028 (2002).
- [13] S. J. Matcher, C. E. Elwell, C. E. Cooper, M. Cope, and D. T. Delpy, *Analyt. Biochem.* **227**(1), 54–68 (1995).
- [14] H. Gray, *Gray's Anatomy*, (Bounty Books, New York, 1977), pp. 1082–1085.
- [15] A. R. Young, *Phys. Med. Biol.* **42**, 789–802 (1997).
- [16] N. Kollias and A. Baqer, *Photochem. Photobiol.* **43**(1), 49–54 (1985).
- [17] M. Doi and S. Tominaga, in: *Color Imaging VIII: Processing, Hardcopy, and Applications*, R. Eschbach and G. G. Marcu, Eds., vol. 5008, (SPIE, 2003) pp. 221–228.
- [18] S. L. Jacques, in: *Advances in Optical Imaging and Photon Migration*, R. R. Alfano and J. G. Fujimoto, Eds., vol. 2, (Optical Society of America, Washington, DC, 1996) pp. 364–370.
- [19] R. Flewelling, in: *The Biomedical Engineering Handbook*, J. Bronzion, Ed., (IEEE Press, Boca Roton, FL, 1981) pp. 1–11.
- [20] R. R. Anderson and J. A. Parrish, *J. Invest. Dermatol.* **77**(1), 13–19 (1981).
- [21] J. T. Whitton and J. D. Everall, *Br. J. Dermatol.* **89**(5), 467–476 (1973).
- [22] M. J. C. Van Gemert, A. J. Welch, W. M. Star, M. Motamedi, and W. F. Cheong, *Lasers Med. Sci.* **2**(4), 295–302 (1987).
- [23] Y. Lee and K. Hwang, *Surg. Radiol. Anat.* **24**(3), 183–189 (2002).
- [24] W. F. Southwood, *Plast. Reconstr. Surg.* **15**, 423–429 (1955).
- [25] V. V. Tuchin, *Tissue Optics: Light Scattering Methods and Instruments for Medical Diagnosis*, (SPIE Press, San Diego, CA, 2007).
- [26] A. Krishnaswamy and G. V. G. Baranoski, in: *Computer Graphics Forum*, (Blackwell Publishing, Inc, 2004) vol. 23, pp. 331–340.
- [27] I. C. Valencia, A. Falabella, R. S. Kirsner, and W. H. Eaglstein, *J. Am. Acad. Dermatol.* **44**(3), 401–424 (2001).
- [28] R. Ruiz-Maldonado and M. de la Luz Orozco-Covarubias, *Semin. Cutan. Med. Surg.* **16**(1), 36–43 (1997).
- [29] V. Falanga, D. Margolis, O. Alvarez, M. Auletta, F. Maggiamo, M. Altman, J. Jensen, M. Sabolinski, and J. Hardin-Young, *Arch. Dermatol.* **134**(3), 293 (1998).
- [30] T. J. Phillips and J. S. Dover, *J. Am. Acad. Dermat.* **25**(6), 965–987 (1991).
- [31] B. Sigel, J. Ipsen, and W. R. Felix, *Ann. Surg.* **179**(3), 278–290 (1974).
- [32] T. Dwyer, G. Prota, L. Blizzard, R. Ashbolt, and M. R. Vincensi, *Melanoma Res.* **10**(4), 387–394, (2000).
- [33] T. Kono, A. R. Erçöçen, H. Nakazawa, T. Honda, N. Hayashi, and M. Nozaki, *Ann. Plast. Surg.* **51**(4), 366 (2003).
- [34] R. L. Greenman, S. Panasyuk, X. Wang, T. E. Lyons, T. Dinh, L. Longoria, J. M. Giurini, J. Freeman, L. Khaodhiar, and A. Veves, *Lancet* **366**(9498), 1711–1717 (2005).
- [35] A. Nouvong, B. Hoogwerf, E. Mohler, B. Davis, A. Tajdini, and E. Medenilla, *Diabetes Care* **32**(11), 2056–2061 (2009).
- [36] J. Sandby-Moller, T. Poulsen, and H. C. Wulf, *Acta Derm. Venereol.* **83**(6), 410–413 (2003).
- [37] M. C. Branchet, S. Boisnic, C. Frances, and A. M. Robert, *Gerontology* **36**(1), 28–35 (1990).
- [38] D. E. Barker, *Plast. Reconstr. Surg.* **7**, 115–116 (1951).
- [39] T. Gambichler, J. Huyn, N. S. Tomi, G. Moussa, C. Moll, A. Sommer, P. Altmeyer, and K. Hoffmann, *Photochem. Photobiol.* **82**(4), 1103–1107 (2006).
- [40] J. Lock-Andersen, P. Therkildsen, O. F. de Fine, M. Gniadecka, K. Dahlstrøm, T. Poulsen, and H. C. Wulf, *Photodermatol. Photoimmunol. Photomed.* **13**(4), 153 (1997).
- [41] T. Gambichler, R. Matip, G. Moussa, P. Altmeyer, and K. Hoffmann, *J. Dermatol. Sci.* **44**(3), 145–152 (2006).
- [42] P. P. Guastalla, V. I. Guerci, A. Fabretto, F. Faletta, D. L. Grasso, E. Zocconi, D. Stefanidou, P. D'Adamo, L. Ronfani, M. Montico, M. Morgutti, and P. Gasparini, *Radiology* **251**(1), 280–286 (2009).
- [43] D. J. Faber and T. G. van Leeuwen, *Opt. Lett.* **34**(9), 1435–1437 (2009).
- [44] D. J. Faber, E. G. Mik, M. C. G. Aalders, and T. G. van Leeuwen, *Opt. Lett.* **30**(9), 1015–1017 (2005).
- [45] K. M. Katika and L. Pilon, *Appl. Opt.* **45**(17), 4174–4183 (2006).
- [46] H. Zeng, C. E. MacAulay, B. Palcic, and D. I. McLean, *Adv. Laser Light Spectrosc. Diagn. Cancer Dis.* **2135**, 94–104 (1994).
- [47] L. Wang and S. L. Jacques, “Monte Carlo modeling of light transport in multi-layered tissues in standard C”, last accessed 3/31/2009, <http://labs.seas.wustl.edu/bme/Wang/mcr5/Mcman.pdf>.
- [48] Z. Guo and K. Kim, *Appl. Opt.* **42**(16), 2897–2905 (2003).
- [49] Y. S. Fawzi, A. B. M. Youssef, M. H. El-Batanony, and Y. M. Kadah, *Appl. Opt.* **42**(31), 6398–6411 (2003).
- [50] A. Kienle, M. S. Patterson, N. Dögnitz, G. Wagnières, and H. van den Bergh, *Appl. Opt.* **37**(4), 779–791 (1998).
- [51] A. Kienle, T. Glanzmann, G. Wagnières, and H. Van den Bergh, *Appl. Opt.* **37**(28), 6852–6862 (1998).
- [52] L. O. Svaasand, L. T. Norvang, E. J. Fiskerstrand, E. K. S. Stopps, M. W. Berns, and J. S. Nelson, *Lasers Med. Sci.* **10**(1), 55–65 (1995).
- [53] M. F. Modest, *Radiative Heat Transfer*, (Academic Press, San Diego, CA, 2003).
- [54] G. Yoon, S. A. Prahl, and A. J. Welch, *Appl. Opt.* **28**(12), 2250–2255 (1989).

- [55] G. Mantis and G. Zonios, *Appl. Opt.* **48**(18), 3490–3496 (2009).
- [56] D. Yudovsky and L. Pilon, *Appl. Opt.* **48**(35), 6670–6683 (2009).
- [57] N. Tsumura, D. Kawazoe, T. Nakaguchi, N. Ojima, and Y. Miyake, *Opt. Rev.* **15**(6), 292–294 (2008).
- [58] Q. Liu and N. Ramanujam, *Appl. Opt.* **45**(19), 4776–4790 (2006).
- [59] C. M. Gardner, S. L. Jacques, and A. J. Welch, *Lasers Surg. Med.* **18**(2), 129–138 (1996).
- [60] J. Wu, F. Partovi, M. S. Field, and R. P. Rava, *Appl. Opt.* **32**(7), 1115–1121 (1993).
- [61] D. Yudovsky and L. Pilon, *Appl. Opt.* **49**(10), 1707–1719 (2010).
- [62] C. Magnain, M. Elias, and J. M. Frigerio, *J. Opt. Soc. Am. A* **25**(7), 1737–1743 (2008).
- [63] N. Terada, K. Ohnishi, M. Kobayashi, and T. Kunitomo, *Int. J. Thermophys.* **7**(5), 1101–1113 (1986).
- [64] J. A. Jacquez, W. McKeehan, J. Huss, J. M. Dimitroff, and H. F. Kuppenheim, *J. Opt. Soc. Am.* **45**(10), 781–784 (1955).
- [65] H. F. Kuppenheim and R. R. Heer, *J. Appl. Physiol.* **4**(10), 800–806 (1952).
- [66] M. J. C. Van Gemert, S. L. Jacques, H. Sterenborg, and W. M. Star, *IEEE Trans. Biomed. Engin.* **36**(12), 1146–1154 (1989).
- [67] V. V. Tuchin, S. R. Utz, and I. V. Yaroslavsky, *Opt. Engin.* **33**, 3178–3188 (1994).
- [68] I. V. Meglinski and S. J. Matcher, *Physiol. Meas.* **23**, 741–753 (2002).
- [69] T. Sarna and R. C. Sealy, *Photochem. Photobiol.* **39**(1), 69–74 (1984).
- [70] S. Prahl, “Optical absorption of hemoglobin”, World Wide Web: <http://omlc.ogi.edu/spectra/hemoglobin/>, 2002.
- [71] A. N. Yaroslavsky, A. V. Priezzhev, J. R. I. V. Yaroslavsky, and H. Battarbee, in: *Handbook of Optical Biomedical Diagnostics*, V. V. Tuchin, Ed., (SPIE Publications, Bellingham, WA, 2002), pp. 169–216.
- [72] S. Wray, M. Cope, D. T. Delpy, J. S. Wyatt, and E. O. Reynolds, *Biochim. Biophys. Acta – Bioenerg.* **933**(1), 184–192 (1988).
- [73] A. P. Harris, M. J. Sendak, R. T. Donham, M. Thomas, and D. Duncan, *J. Clin. Monit. Comput.* **4**(3), 175–177 (1987).
- [74] S. Takatani and M. D. Graham, *IEEE Trans. Biomed. Engin.* **26**(12), 656–664 (1979).
- [75] J. R. Mourant, J. P. Freyer, A. H. Hielscher, A. A. Eick, D. Shen, and T. M. Johnson, *Appl. Opt.* **37**(16), 3586–3593 (1998).
- [76] J. R. Mourant, T. Fuselier, J. Boyer, T. M. Johnson, and I. J. Bigio, *Appl. Opt.* **36**(4) 949–957 (1997).
- [77] R. Graaff, J. G. Aarnoudse, J. R. Zijp, P. M. A. Sloot, F. F. M. de Mul, J. Greve, and M. H. Koelink, *Appl. Opt.* **31**(10), 1370–1376 (1992).
- [78] A. N. Bashkatov, E. A. Genina, V. I. Kochubey, and V. V. Tuchin, *J. Phys.* **38**(15), 2543–2555 (2005).
- [79] T. L. Troy and S. N. Thennadil, *J. Biomed. Opt.* **6**, 167–176 (2001).
- [80] M. J. C. van Gemert and W. M. Star, *Lasers Life Sci.* **1**(287–298), 98 (1987).
- [81] R. I. Kelly, R. Pearse, R. H. Bull, J. L. Leveque, J. de Rigal, and P. S. Mortimer, *J. Amer. Acad. Dermatol.* **33**(5), 749–756 (1995).
- [82] E. Salomatina, B. Jiang, J. Novak, and A. N. Yaroslavsky, *J. Biomed. Opt.* **11**, 064026 (2006).
- [83] C. R. Simpson, M. Kohl, M. Essenpreis, and M. Cope, *Phys. Med. Biol.* **43**, 2465–2478 (1998).
- [84] E. K. Chan, B. Sorg, D. Protsenko, M. O’Neil, M. Motamedi, and A. J. Welch, *IEEE J. Sel. Top. Quant. Electron.* **2**(4), 943–950 (1996).
- [85] T. Dwyer, H. K. Muller, L. Blizzard, R. Ashbolt, and G. Phillips, *Cancer Epidemiol. Biomarkers Prev.* **7**(3), 203–206 (1998).